Polaron Origin for Anharmonicity of the Axial Oxygen in $YBa_2Cu_3O_7$

J. Mustre de Leon, I. Batistić, A. R. Bishop, S. D. Conradson, and S. A. Trugman
Los Alamos National Laboratory, Los Alamos, New Mexico 87545
(Received 29 October 1991)

We present exact diagonalization results of an electron-phonon model Hamiltonian for the O(4)-Cu(1)-O(4) cluster in $YBa_2Cu_3O_7$. For large enough electron–infrared-phonon coupling the motion of holes and ions becomes strongly correlated, i.e., polaronic, leading to a double-well structure for the infrared mode, as encountered in x-ray-absorption fine structure. In contrast, the associated Raman mode shows a single-well behavior even for large electron–Raman-phonon coupling. The appearance of polarons accompanies nonadiabatic behavior yielding optical spectroscopy predictions differing from those obtained from harmonic or anharmonic lattice dynamics models.

PACS numbers: 74.30.−e, 61.10.Lx, 63.20.Ry

Although the microscopic origin of high-temperature superconductivity in copper-oxide-based materials is still a matter of debate, several experiments have shown the existence of structural instabilities and anomalies [1–9], suggesting the importance of the lattice. Various theoretical models [10–14] have specifically suggested the presence of anharmonicity associated with the motion of the oxygen atoms. A fundamental issue is the ability of these models to *correlate* structural and optical signatures.

Elsewhere, we have presented x-ray-absorption fine-structure (XAFS) results which indicate that the Cu(1)-O(4) bonds in $YBa_2Cu_3O_7$ [i.e., c axis, with Cu(1) a chain copper and O(4) an axial bridging oxygen] show a double-well structure which changes in the vicinity of T_c [1], and as a function of oxygen content and doping [2]. Pair-radial-distribution-function analysis of neutron diffraction data has also shown the existence of two axial oxygen positions in $Tl_2Ba_2CaCu_2O_8$ [4]. These structural studies indicate dynamical oscillations between these two positions, which cannot be explained in terms of harmonic phonons and should be reflected in optical measurements of the normal modes with projections onto the Cu(1)-O(4) vibrations. The 505-cm^{-1} A_g Raman mode in $YBa_2Cu_3O_7$ shows a hardening, from 506 cm^{-1} at 100 K to 509 cm^{-1} at 50 K, and a concomitant increase in the linewidth of 2 cm^{-1} [5,6]. These results have been interpreted as originating in the change of the *harmonic* phonon self-energy [15] due to coupling to the superconducting pairs [5–7], assuming a superconducting gap of $440 < 2\Delta < 500$ cm^{-1}. This model has been purported to imply the absence of anharmonicity in this phonon mode [8], a claim also suggested by band-structure total-energy calculations [16]. In contrast to the Raman spectroscopy results, infrared absorption studies of the associated 585-cm^{-1} mode indicate a *softening* from 590 cm^{-1} at 100 K to 584 cm^{-1} at 50 K and an increase in the intensity by a factor of 2 for the same temperature values [9]. Photoinduced infrared absorption in $YBa_2Cu_3O_{6.3}$ and $Tl_2Ba_2Ca_{1-x}Gd_xCu_2O_8$ [17] have also suggested a double-well potential structure, in agreement with XAFS results [1,2].

We have performed an exact diagonalization [18] of an electron-phonon model Hamiltonian [19], representing c-axis lattice-electron coupling [20], considering both infrared and Raman active vibrations in an isolated O(4)-Cu(1)-O(4) cluster in $YBa_2Cu_3O_7$. This model allows us to (i) understand the origin of the differing behavior of the infrared and Raman modes and reconcile apparent conflicts between Raman spectroscopy and XAFS results; (ii) reveal an underlying polaronic origin for the XAFS double well; and (iii) explore the validity of effective lattice dynamics in correlating structural and optical results.

The cluster Hamiltonian we use is

$$H = H_{\rm el} + H_{\rm ph} + H_{\rm el\text{-}ph}\,, \tag{1}$$

$$H_{\rm el} = \sum_{\sigma,i=1}^{3} \epsilon_i n_{i\sigma} + U\sum_{i=1}^{3} n_{i\uparrow} n_{i\downarrow} + t\sum_{\sigma} (c_{1\sigma}^{\dagger} c_{2\sigma} + c_{2\sigma}^{\dagger} c_{3\sigma}) + \text{H.c.}\,, \tag{1a}$$

$$H_{\rm ph} = \hbar\omega_{\rm ir}^{0} b_{\rm ir}^{\dagger} b_{\rm ir} + \hbar\omega_{R}^{0} b_{R}^{\dagger} b_{R}\,, \tag{1b}$$

$$H_{\rm el\text{-}ph} = -\tilde{\lambda}_R u_R \sum_{\sigma} (n_{1\sigma} - 2n_{2\sigma} + n_{3\sigma}) - \tilde{\lambda}_{\rm ir} u_{\rm ir} \sum_{\sigma} (n_{3\sigma} - n_{1\sigma})\,. \tag{1c}$$

Here, $n_{i\sigma} = c_{i\sigma}^{\dagger} c_{i\sigma}$ denotes the number operator for holes of spin σ at site i; $i = 1,3$ indicates the lower and upper O(4) sites, and $i = 2$ the Cu(1) site, with site energies ϵ_i ($\epsilon_1 = \epsilon_3 \neq \epsilon_2$), hopping amplitude t, and on-site repulsion U. The phonon part of the Hamiltonian (1b) consists of harmonic Raman and infrared oscillators with creation operators $b_R^{\dagger}$ and $b_{\rm ir}^{\dagger}$ and bare frequencies ω_R^0 and $\omega_{\rm ir}^0$, respectively. These operators are related to the Raman coordinate by $u_R = (\hbar/2m_O\omega_R^0)^{1/2}(b_R^{\dagger} + b_R) = (x_3 - x_1)/\sqrt{2}$, and to the infrared coordinate by

$$u_{\rm ir} = \left(\frac{\hbar}{2m_O\omega_{\rm ir}^0}\right)^{1/2} (b_{\rm ir}^{\dagger} + b_{\rm ir}) = \frac{x_1 + x_3 - (2m_O/m_{\rm Cu})x_2}{(2 + 4m_O/m_{\rm Cu})^{1/2}}\,.$$

Here, x_1 (x_3) denotes the lower (upper) O(4) coordinate and x_2 the Cu(1) coordinate measured from their equilibrium positions, and $m_{\rm Cu}$ (m_O) is the Cu(1) [O(4)] mass.

The interaction term (1c) reflects the fact that for holes added at the Cu(1) site the Cu(1)-O(4) attraction is stronger, while for holes added at the O(4) sites the attraction is weaker, favoring a longer Cu(1)-O(4) bond length. We consider coupling of these Cu(1)-O(4) charge fluctuations to both the infrared and Raman modes. For simplicity we consider only coupling between phonons and diagonal electronic terms. This local approach to describing the oxygen polarizability should be compared with *anharmonic* electron-phonon coupling models [21], which lead to a correlated double-well and electron-multiphonon coupling [10]. In the present approach the anharmonicity is not present in the bare phonon Hamiltonian, but is generated by sufficiently strong linear electron-phonon coupling.

We assume two holes of different spin (singlet), leading to the cluster states (a) $O(4)^{2-}$-$Cu(1)^{2+}$-$O(4)^{1-}$ and (b) $O(4)^{1-}$-$Cu(1)^{2+}$-$O(4)^{2-}$, consistent with near-edge x-ray-absorption experiments [22]. The state $O(4)^{2-}$-$Cu(1)^{3+}$-$O(4)^{2-}$ is found to be important as an intermediate state for tunneling between states (a) and (b). All other states with the same total charge and S_z are also included in the Hilbert space. More precisely, one expects a cluster configuration with an average number of holes between 1 and 2 for $YBa_2Cu_3O_7$, the two-hole cluster being an adequate description provided that the parameters entering in Eq. (1a) are viewed as effective parameters, including transverse degrees of freedom.

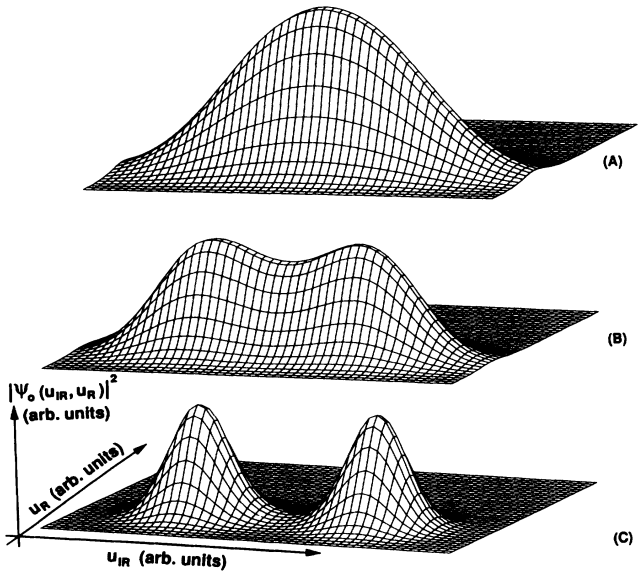

FIG. 1. Squared many-body ground-state wave function of the cluster as a function of the Raman (u_R) and infrared (u_{ir}) coordinates for (a) $\lambda_{ir}=0.10$ eV, (b) $\lambda_{ir}=0.12$ eV, and (c) $\lambda_{ir}=0.15$ eV (in all cases $\lambda_R=0.10$ eV). We find that when the phonon coordinate is at the left bump, the extra hole is predominantly on the leftmost oxygen, and vice versa. The scale of the coordinates is fixed to be 3 times the root-mean-square fluctuation of the wave function, and therefore it is different for the three panels.

We exactly diagonalize [18] Eq. (1) for the ground and low-lying excited states in a basis of 14400 states using a Lanczos algorithm. The basis includes states of two holes on the three sites, 40 harmonic infrared phonons, and 40 harmonic Raman phonons. For the parameters in Eq. (1a) we use $\epsilon_{1,3}=+0.5$ eV, $\epsilon_2=-0.5$ eV, $t=0.5$ eV, and $U=7.0$ eV. In Eq. (1b) we use $\omega_{ir}^0=600$ cm^{-1} and $\omega_R^0=500$ cm^{-1}, whose ratio is determined by m_O/m_{Cu} [23]. We consider the range $\lambda_R=\tilde{\lambda}_R(\hbar/2m_O\omega_R^0)^{1/2}=0$–$0.25$ eV, and $\lambda_{ir}=\tilde{\lambda}_{ir}(\hbar/2m_O\omega_{ir}^0)^{1/2}=0$–$0.20$ eV. Different parameter values result in different values of λ_R and λ_{ir} at which the characteristic anharmonic behavior discussed below develops.

In Fig. 1 we present the squared many-body ground-state wave function plotted as a function of the infrared (u_{ir}) and Raman (u_R) coordinates, for increasing values of λ_{ir} at a fixed representative value of $\lambda_R=0.10$ eV. In this case we have summed over the electronic degrees of freedom, i.e., the probability is for given phonon coordinates regardless of the electron coordinates. As λ_{ir} increases the wave function deviates from a Gaussian shape, a double-peak structure begins developing for $\lambda_{ir}\cong 0.12$ eV, and the two peaks are completely separated for $\lambda_{ir}\geq 0.15$ eV (Table I). The peak in the Raman coordinate shifts from the (bare) equilibrium position $u_R=0$ as λ_R increases [20], but no double-well structure develops, even for $\lambda_R=0.20$ eV.

The above behavior is entirely intuitive, since the configuration *short*-Cu(1)-upper-O(4) bond and *long*-Cu(1)-lower-O(4) bond is expected to be degenerate with the configuration *long*-Cu(1)-upper-O(4) bond and a *short*-Cu(1)-lower-O(4), while a *symmetric* stretch or contraction of both bonds, relevant for the Raman mode, will change the total energy of the cluster differently, as found in band-structure calculations [16]. Note that we are discussing charge transfer within the cluster, and not between the cluster and the plane.

We found that $\lambda_R=0.10$ eV and $\lambda_{ir}=0.13$ eV lead to O(4) site splitting of ~ 0.125 Å, in agreement with the experimental value of ~ 0.13 Å of Ref. [1]. The XAFS

TABLE I. Separation, tunneling frequency, and infrared phonon expectation value as a function of λ_{ir} ($\lambda_R=0.10$ eV).

λ_{ir} (eV)	Separation (Å)	$\hbar\omega_T$ (cm^{-1})	$\langle N_{ph}^{ir}\rangle$
0.10 (single well)	...	235	0.3
0.12	0.050	90	0.8
0.13	0.125	52	1.5
0.15	0.174	8	3.0
0.20	0.258	0.01	6.4
0.25	0.330	4.4×10^{-6}	10.5
EXAFS double well[a]	0.130	100	...

[a]Reference [1].

splitting, Δx, is related to the separation between the two maxima of the many-body state wave function, Δu_{ir}, by $\Delta x=(1+2m_O/m_{Cu})^{1/2}\Delta u_{ir}/\sqrt{2}$. The exact many-body tunneling frequency, $\hbar\omega_T$, for this cluster is the difference between the first excited-state and ground-state energies. For the values mentioned above, we obtain $\hbar\omega_T\sim 52$ cm^{-1} compared with the tunneling frequency implied by the structural studies [1] $\hbar\omega_T\sim 100$ cm^{-1} (away from T_c) (Table I). We consider this good agreement in view of the simplicity of the model and the exponential dependence of the tunneling frequency on the assumed mass. Further tuning of parameters (including λ_R) is not warranted without more refined data.

A full description of the many-body states which includes both phonon and electron degrees of freedom leads to the following picture as λ_{ir} is varied around the experimentally relevant values above: For small values of λ_{ir} the tunneling of holes between the O(4) sites occurs on a time scale much faster than ionic motion, allowing the use of the adiabatic approximation and leading to quasiharmonic phonon behavior characterized by a simple shift in the phonon frequency, and phonon expectation values $\ll 1$ (Table I). As λ_{ir} increases the motion of the holes couples to the phonons leading to the experimentally relevant polaronic behavior [24], i.e., two equilibrium positions depending on the location of the O(4) hole. For large values of λ_{ir} the effective tunneling of holes becomes very slow and the first two many-body wave functions can be represented by the symmetric

$$|\Psi_0\rangle=(|110\rangle|-z_{ir}\rangle|-z_R\rangle+|011\rangle|z_{ir}\rangle|-z_R\rangle)/\sqrt{2}$$

and antisymmetric

$$|\Psi_1\rangle=(|110\rangle|-z_{ir}\rangle|-z_R\rangle-|011\rangle|z_{ir}\rangle|-z_R\rangle)/\sqrt{2}$$

states. Here, $|n_1n_2n_3\rangle$ denotes the hole occupation at each site and $|z\rangle$ the ground-state wave function of a harmonic oscillator centered at z (a coherent state). In this "antiadiabatic" limit the holes are nearly "frozen" (incipient ferroelectricity), the ions oscillate harmonically with respect to the shifted equilibrium positions [25], and the (unshifted) phonon expectation value increases significantly (Table I). It is very intriguing that the best fit to XAFS results places us in the *intermediate* λ_{ir} regime.

These results demonstrate how the charge-transfer–phonon coupling generates a double-well structure consistent with the structural results derived from XAFS, reconcile this with infrared and Raman observations, and explicitly show the underlying polaronic origin of such double-well behavior. Although a lattice dynamics model which uses a rigid double well derived by integrating out electronic degrees of freedom is successful in describing the structural results [1], we need to assess whether such a model will lead to optical spectroscopy predictions similar to the ones calculated with the full model, Eq. (1). To this end we have calculated the imaginary part of the dielectric constant [20,26]:

$$\mathrm{Im}\epsilon(\omega)=\sum_j \frac{S_j\omega_j^2}{\omega_j^2-\omega_2-i\omega\gamma}. \tag{2}$$

Here, j labels the many-body states with energies ω_j and we assume the same width, $\gamma=17$ cm^{-1}, for all states [20,26]. The spectral weight of each transition is given by the square of the dipole matrix element between the ground state and the jth state, $S_j=|\langle j|p|0\rangle|^2$, with a dipole operator

$$p=-\left[8\left(1+\frac{2m_O}{m_{Cu}}\right)\right]^{1/2}u_{ir}+\sum_\sigma\left(R_0-\frac{u_R}{\sqrt{2}}\right)(n_{3\sigma}-n_{1\sigma})$$
$$+\sum_\sigma\left(1+\frac{2m_O}{m_{Cu}}\right)^{1/2}\frac{u_{ir}}{\sqrt{2}}(n_{3\sigma}+n_{1\sigma}), \tag{3}$$

where R_0 denotes the equilibrium distance of the Cu(1)-O(4) bond (1.87 Å). Figure 2 plots the energies of the first four many-body states with nonzero oscillator strengths. In the weak coupling limit, state A is the excited state containing one infrared phonon, while in the strong coupling limit (slow tunneling), this state is the antisymmetric state $|\Psi_1\rangle$ mentioned above. State B has one infrared and one Raman phonon in the weak coupling limit, and one Raman phonon (in addition to the coherent state displacement) in the strong coupling limit. State C has one infrared and two Raman phonons in weak coupling, and one infrared phonon in strong coupling. Finally, state D has three infrared phonons in weak coupling, and two Raman phonons in strong coupling. In the strong coupling limit all these states can be associated with excited states of displaced harmonic oscillators.

The inset of Fig. 2 is a plot of $\mathrm{Im}\epsilon(\omega)$ for $\lambda_{ir}=0.13$ eV

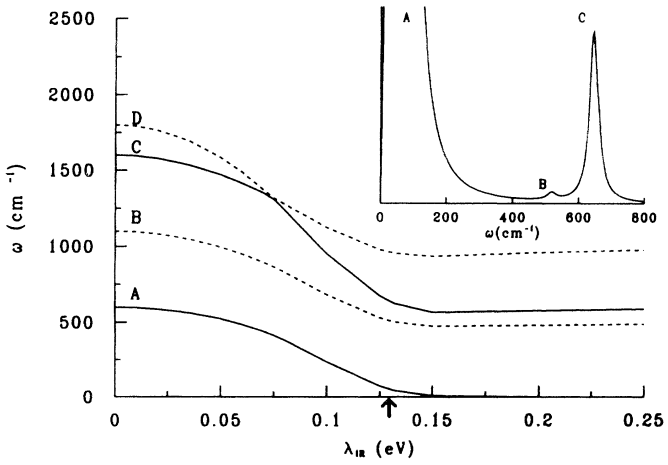

FIG. 2. Energies of the first four infrared allowed transitions as a function of λ_{ir}. The Raman coupling is $\lambda_R=\lambda_{ir}$ for $\lambda_{ir}\leq 0.10$ eV, and $\lambda_R=0.10$ eV for $\lambda_{ir}\geq 0.10$ eV. There is an avoided crossing of the highest two levels. The arrow indicates the experimentally relevant $\lambda_{ir}=0.13$ eV (see text). Inset: $\mathrm{Im}\epsilon(\omega)$ for $\lambda_R=0.10$, $\lambda_{ir}=0.13$ eV. The height of peak A is ~ 10 times larger than that of peak C; cf. Fig. 4 in Ref. [20].

and $\lambda_R = 0.10$ eV, the value which yielded the best consistency with XAFS results. For small values of λ_{ir} the peak associated with state A is shifted from ω_{ir}^0, as expected in perturbative treatments of anharmonicity. For *moderate* values of λ_{ir} (the expected polaronic regime) peak A, which corresponds to the tunneling frequency, shifts to low frequency, and *two* peaks appear in the region $\omega \sim 450$–600 cm^{-1}, which are states B and C. For large values of λ_{ir} ("antiadiabatic" regime), the intensity of the peak associated with state B becomes negligible, leaving a single peak converging to the original bare infrared frequency. This behavior originates in the "freezing" of holes at the oxygen sites, resulting in harmonic oscillations (with the bare frequency) around the new equilibrium position, and leading to a negligible amplitude for both holes to reside on the Cu(1) atom in the ground state, an amplitude which allows the excitation of the Raman mode (B). We emphasize that our analysis of the model Eq. (1) is exact, aside from small truncation errors from excluding phonons beyond the first 40 of each type. Thus, the anharmonic features predicted are not limited by random-phase [19] or adiabatic elimination approximations, which are inappropriate in this small O(4)-Cu(1)-O(4) cluster. Consequently, effects beyond simple single-particle anharmonic lattice dynamics are anticipated. Calculations (within the dipole approximation) using a rigid double-well potential based on the XAFS results only show peaks associated with states A and C.

Although this calculation of the infrared spectra for a simple cluster is not expected to lead to a quantitative comparison with experiment, there are some encouraging systematics: (i) The large spectral weight of the low-frequency feature might be related to the enhanced intensity of the 154-cm^{-1} mode compared with bare lattice dynamics calculations [20]; and (ii) in Refs. [20] and [26] there is evidence for strong asymmetry in the line shape of the 585-cm^{-1} mode, which could be related with the split peak predicted in our calculation. This feature is very close to the experimental peak at ~ 585 cm^{-1}. A calculation of the Raman spectra will be presented elsewhere.

In summary, we have developed an electron-phonon model which explicitly shows that the coupling between c-axis phonons and charge transfer between Cu(1) and O(4) ions generates a double well for the 585-cm^{-1} infrared mode while it leads to a shifted single well for the associated Raman mode. These results reconcile optical and structural observations. This model predicts multiphonon and nonadiabatic effects, not contained in effective harmonic or anharmonic lattice dynamics calculations, which should be observable via optical spectroscopy. Finally, we have shown that the Cu(1)-O(4) double well has a polaronic tunneling origin [24]—the hole location follows the lattice distortion in the cluster. It is intriguing that the λ_{ir} needed to fit XAFS results lies in the intermediate (polaron tunneling) regime—weaker coupling implies fast bare electrons, whereas stronger coupling would, for an extended system, result in a nearly frozen local ferroelectric dipole. The influence of this dynamical polarizability "pump" on superconducting pairing has been suggested elsewhere [27].

We would like to thank A. Bussmann-Holder and Y. Yacoby for stimulating discussions, and the Los Alamos Advanced Computing Laboratory for the use of a CONVEX C-220 computer. This work was supported by the U.S. Department of Energy.

[1] S. D. Conradson *et al.*, Science **248**, 1394 (1990); J. Mustre de Leon *et al.*, Phys. Rev. Lett. **65**, 1675 (1990).
[2] J. Mustre de Leon *et al.*, Phys. Rev. B **44**, 2422 (1991).
[3] R. P. Sharma *et al.*, Phys. Rev. Lett. **62**, 2869 (1989).
[4] B. H. Toby *et al.*, Phys. Rev. Lett. **64**, 2414 (1990); T. Egami *et al.*, Physica (Amsterdam) **185-189C**, 867 (1991).
[5] E. Altendorf *et al.*, Physica (Amsterdam) **175C**, 44 (1991).
[6] B. Friedl *et al.*, Solid State Commun. **78**, 291 (1991).
[7] K. F. McCarty *et al.*, Phys. Rev. B **43**, 13751 (1991).
[8] G. Burns *et al.*, Solid State Commun. **75**, 893 (1990).
[9] H. S. Obhi and E. K. Salje, Physica (Amsterdam) **171C**, 547 (1990); B. Güttler *et al.*, J. Phys. Condens. Matter **2**, 8977 (1990).
[10] A. Bussmann-Holder and A. R. Bishop, Phys. Rev. B **44**, 2853 (1991).
[11] K. H. Johnson *et al.*, Mod. Phys. Lett. B **3**, 1367 (1989).
[12] N. M. Plakida *et al.*, Europhys. Lett. **4**, 1309 (1987); J. R. Hardy and J. W. Flocken, Phys. Rev. Lett. **60**, 2191 (1988).
[13] D. P. Clougherty, K. H. Johnson, and M. E. McHenry, Physica (Amsterdam) **162-164C**, 1475 (1989).
[14] Y. Bar-Yam, Phys. Rev. B **43**, 359 (1991).
[15] R. Zeyher and G. Zwicknagl, Solid State Commun. **66**, 617 (1988).
[16] R. E. Cohen *et al.*, Phys. Rev. Lett. **64**, 2575 (1990).
[17] D. Mihailović *et al.*, Phys. Rev. B **44**, 237 (1991).
[18] S. A. Trugman, in *Applications of Statistical and Field Theory Methods to Condensed Matter*, edited by D. Baeriswyl, A. Bishop, and J. Carmelo, NATO Advanced Study Institute Ser. B, Vol. 218 (Plenum, New York, 1990).
[19] I. Batistić *et al.*, Phys. Rev. B **40**, 6896 (1989).
[20] L. Genzel *et al.*, Phys. Rev. B **40**, 2170 (1989).
[21] A. Bussmann *et al.*, Ferroelectrics **25**, 343 (1980); **39**, 12340 (1989).
[22] A. Bianconi *et al.*, Phys. Rev. B **38**, 7196 (1988).
[23] L. D. Landau and E. M. Lifshitz, *Mechanics* (Pergamon, Oxford, 1976), p. 72.
[24] J. Ranninger, Phys. Scr. (to be published); J. Ranninger and U. Thibblin, Phys. Rev. B **45**, 7730 (1992).
[25] R. Micnas, J. Ranninger, and S. Robaszkiewicz, Rev. Mod. Phys. **62**, 113 (1990). S. Aubry *et al.*, *Nonlinear Coherent Structures in Physics, Mechanics and Biological Systems* (Springer, New York, 1989), p. 103.
[26] D. A. Bonn *et al.*, Phys. Rev. B **37**, 1574 (1988).
[27] A. R. Bishop, in *Early and Recent Aspects of Superconductivity*, edited by K. A. Müller and J. G. Bernordz (Springer, New York, 1991).